

Phase-sensitive fiber-based parametric all-optical switch

Josué Parra-Cetina,* Aleš Kumpera, Magnus Karlsson, and Peter A. Andrekson

Fibre Optic Communication Research Centre (FORCE), Photonics Laboratory, Department of Microtechnology and Nanoscience, Chalmers University of Technology, SE-41296, Göteborg, Sweden
*amlcar@chalmers.se

Abstract: We experimentally demonstrate, for the first time, an all-optical switch in a phase-sensitive fiber optic parametric amplifier operated in saturation. We study the effect of phase variation of the signal and idler waves on the pump power depletion. By changing the phase of a 0.9 mW signal/idler pair wave by $\pi/2$ rad, a pump power extinction ratio of 30.4 dB is achieved. Static and dynamic characterizations are also performed and time domain results presented.

©2015 Optical Society of America

OCIS codes: (190.4970) Parametric oscillators and amplifiers; (190.4380) Nonlinear optics, four-wave mixing.

References and links

1. P. W. Smith, "On the role of photonic switching in future communications systems," *IEEE Circuits Dev. Mag.* **3**(3), 9–14 (1987).
2. D. A. B. Miller, "Are optical transistors the logical next step?" *Nat. Photonics* **4**(1), 3–5 (2010).
3. K. E. Stubkjaer, "Semiconductor optical amplifier-based all-optical gates for high-speed optical processing," *IEEE J. Sel. Top. Quantum Electron.* **6**(6), 1428–1435 (2000).
4. S. A. Hamilton, B. S. Robinson, T. E. Murphy, S. J. Savage, and E. P. Ippen, "100 Gb/s optical time division multiplexed networks," *J. Lightwave Technol.* **20**(12), 2086–2100 (2002).
5. H. Soto, J. C. Dominguez, D. Erasme, and G. Guekos, "Demonstration of an all-optical switch using cross-polarization modulation in semiconductor optical amplifiers," *Microw. Opt. Technol. Lett.* **29**(3), 205–208 (2001).
6. S. Nakamura, Y. Ueno, K. Tajima, J. Sasaki, T. Sugimoto, T. Kato, T. Shimoda, M. Itoh, H. Hatakeyama, T. Tamanuki, and T. Sasaki, "Demultiplexing of 168-Gb/s data pulses with a hybrid-integrated symmetric Mach-Zehnder all-optical switch," *IEEE Photonics Technol. Lett.* **12**(4), 452–457 (2000).
7. J. Kurumida, H. Uenohara, and K. Kobayashi, "All-optical label and payload separation using a self-switching technique of a SOA-MZI," in *European Conference on Optical Communications* (IEEE, 2006), pp. 1–2.
8. J. P. Wang, B. S. Robinson, S. J. Savage, S. A. Hamilton, E. P. Ippen, R. Mu, H. Wang, J. Sarathy, and B. B. Stefanov, "Efficient performance optimization of SOA-MZI devices," *Opt. Express* **16**(5), 3288–3292 (2008).
9. D. J. Hagan, Z. Wang, G. Stegeman, E. W. Van Stryland, M. Sheik-Bahae, and G. Assanto, "Phase-controlled transistor action by cascading of second-order nonlinearities in KTP," *Opt. Lett.* **19**(17), 1305–1307 (1994).
10. P. Sethi and S. Roy, "All-optical ultrafast switching in 2x2 silicon microring resonators and its application to reconfigurable DEMUX/MUX and reversible logic gates," *J. Lightwave Technol.* **32**(12), 2173–2180 (2014).
11. Y. Vlasov, W. M. J. Green, and F. Xia, "High-throughput silicon nanophotonic wavelength-insensitive switch for on-chip optical networks," *Nat. Photonics* **2**(4), 242–246 (2008).
12. K. Nozaki, T. Tanabe, A. Shinya, S. Matsuo, T. Sato, H. Taniyama, and M. Notomi, "Sub-femtojoule all-optical switching using a photonic crystal nanocavity," *Nat. Photonics* **4**(7), 477–483 (2010).
13. L. Lengle, M. Gay, A. Bazin, I. Sagnes, R. Braive, P. Monnier, L. Bramerie, T-N. Nguyen, C. Pareige, R. Madec, J-C. Simon, R. Raj, and F. Raineri, "Fast all-optical 10GB/s NRZ wavelength conversion and power limiting function using hybrid InP on SOI nanocavity," in *European Conference on Optical Communications* (IEEE, 2012), paper We.2 E.5.
14. E. Yüce, G. Ctistis, J. Claudon, E. Dupuy, R. D. Buijs, B. de Ronde, A. P. Mosk, J. M. Gérard, and W. L. Vos, "All-optical switching of a microcavity repeated at terahertz rates," *Opt. Lett.* **38**(3), 374–376 (2013).
15. D. Englund, A. Majumdar, M. Bajcsy, A. Faraon, P. Petroff, and J. Vučković, "Ultrafast photon-photon interaction in a strongly coupled quantum dot-cavity system," *Phys. Rev. Lett.* **108**(9), 093604 (2012).
16. P. A. Andrekson, H. Sunnerud, S. Oda, T. Nishitani, and J. Yang, "Ultrafast, atto-Joule switch using fiber-optic parametric amplifier operated in saturation," *Opt. Express* **16**(15), 10956–10961 (2008).
17. R. Nissim, A. Pejkić, E. Myslivets, B. P. Kuo, N. Alic, and S. Radic, "Ultrafast optical control by few photons in engineered fiber," *Science* **345**(6195), 417–419 (2014).

18. A. Pejkic, R. R. Nissim, E. Myslivets, A. O. J. Wiberg, N. Alic, and S. Radic, "All-optical switching in a highly efficient parametric fiber mixer: design study," *Opt. Express* **22**(19), 23512–23527 (2014).
19. G. P. Agrawal and M. J. Potasek, "Nonlinear pulse distortion in single-mode optical fibers at the zero-dispersion wavelength," *Phys. Rev. A* **33**(3), 1765–1776 (1986).
20. P. Beaud, W. Hodel, B. Zysset, and H. P. Weber, "Ultrashort pulse propagation, pulse breakup, and fundamental soliton formation in a single-mode optical fiber," *IEEE J. Quantum Electron.* **23**(11), 1938–1946 (1987).
21. C. McKinstrie and S. Radic, "Phase-sensitive amplification in a fiber," *Opt. Express* **12**(20), 4973–4979 (2004).
22. C. Lundström, B. Corcoran, M. Karlsson, and P. A. Andrekson, "Phase and amplitude characteristics of a phase-sensitive amplifier operating in gain saturation," *Opt. Express* **20**(19), 21400–21412 (2012).
23. R. Tang, J. Lasri, P. S. Devgan, V. Grigoryan, P. Kumar, and M. Vasilyev, "Gain characteristics of a frequency nondegenerate phase-sensitive fiber-optic parametric amplifier with phase self-stabilized input," *Opt. Express* **13**(26), 10483–10493 (2005).
24. C. Lundström, R. Malik, L. Grüner-Nielsen, B. Corcoran, S. L. I. Olsson, M. Karlsson, and P. A. Andrekson, "Fiber optic parametric amplifier with 10 dB net gain without pump dithering," *IEEE Photonics Technol. Lett.* **25**(3), 234–237 (2013).
25. S. Oda, H. Sunnerud, and P. A. Andrekson, "High efficiency and high output power fiber-optic parametric amplifier," *Opt. Lett.* **32**(13), 1776–1778 (2007).
26. P. Kylemark, H. Sunnerud, M. Karlsson, and P. A. Andrekson, "Semi-analytic saturation theory of fiber optical parametric amplifiers," *J. Lightwave Technol.* **24**(9), 3471–3479 (2006).
27. R. R. Nissim, A. Pejkic, E. Myslivets, N. Alic, and S. Radic, "Origin of non-reciprocal response in fiber optics parametric amplifiers," *J. Lightwave Technol.* **33**(2), 495–502 (2015).
28. Z. Tong, A. O. J. Wiberg, E. Myslivets, B. P. P. Kuo, N. Alic, and S. Radic, "Spectral linewidth preservation in parametric frequency combs seeded by dual pumps," *Opt. Express* **20**(16), 17610–17619 (2012).
29. K. Inoue and T. Mukai, "Signal wavelength dependence of gain saturation in a fiber optical parametric amplifier," *Opt. Lett.* **26**(1), 10–12 (2001).

1. Introduction

Optical switches have for two decades received much attention as a technology driving future optical network devices and systems. Switching signals fully in the optical domain promises a huge performance leap in terms of bitrate, bandwidth and energy efficiency [1,2].

Some of the first demonstrations of all-optical switching were proposed using in-line semiconductor optical amplifiers (SOAs). In these works, different nonlinear phenomena inside a SOA were exploited, such as cross polarization modulation (XPM), cross gain modulation (XGM) and four-wave mixing (FWM) [3–5]. The control signal had at least one order of magnitude higher than the signal to be switched, and provided in the best scenarios extinction ratios (ERs) of up to 30 dB [5]. Another option was to use SOAs with interferometers [6–8], which implied incorporating two or more SOAs. The switching operation was then achieved by the influence of a strong control signal introduced into one arm of the interferometer configuration causing depletion of carriers in the SOA, resulting in gain saturation and modification of the refractive index. Optical switches based on SOAs offer a hybrid solution as an electrical bias is required to supply carriers acting as a medium for interaction between photons. For this reason, the performance of such devices depends mainly on the carrier dynamics limiting their usage to few tens of gigahertz with current state-of-the-art technologies. When SOAs are combined with interferometers their ER is improved at the expense of more complex device layout and an increase in the cost due to the additional biasing electrical components needed.

Ultrafast switching operations with speeds beyond the limits of electrical devices can only be achieved through an all-optical approach. In this context, different approaches have recently been demonstrated using nonlinear effects in $\chi^{(2)}$ (2nd-order susceptibility) and $\chi^{(3)}$ (3rd-order susceptibility) media [9–18]. Some of these techniques have been briefly compared providing their advantages and disadvantages [18]. The work presented in [9] was different from the others, in that second harmonic generation (SHG) in a Potassium Titanyl Phosphate (KTP) crystal was used to modulate a strong wave by variations of the relative phase of the interacting waves. However, the configuration required special alignment and control as well as using interacting waves at wavelengths of 530 and 1060 nm outside the telecom bands. Some of the most successful and promising devices are the ones harnessing Kerr nonlinearities ($\chi^{(3)}$) in a waveguide, e.g., parametric processes based on FWM. The

mechanism has ultrafast (femtosecond response) and is highly efficient in a medium with a large product of nonlinearity and interaction length. In this regard, silica fibers are the ideal physical platform. All-optical switching approaches using parametric amplification in a phase insensitive (PI) regime in a highly nonlinear fiber (HNLF) have been reported achieving extinction ratios of up to 17 dB [16–18]. In the three works, the control of a strong signal was demonstrated by using a low intensity (few photons) signal. In [16], a standard HNLF was utilized whilst in [17,18] an engineered fiber enabled an efficient control of the fiber dispersion at a sub-nanometer scale which allowed even fewer photons to control the strong light signal. However, in both works pulses were used as the interacting input waves which could give rise to walk-off and soliton pulse compression limiting the performance of the switch in terms of ER. This required a careful selection of the parameters of the interacting waves (wavelengths and pulse-width) as a function of the zero dispersion wavelength (ZDW) of the medium [18–20]. On the other hand, it is worth noting that not only the intensity of an optical signal can provide information, but also the phase, which could also be used to control the output waves in a parametric amplifier, as demonstrated in [9]. It is well-known that under certain conditions, fiber optic parametric amplifiers (FOPAs) can also work in a phase sensitive (PS) mode which makes the parametric process dependent on the intensity and phase of the interacting waves [21]. In [22] a study of the phase and amplitude characteristics of a phase-sensitive amplifier (PSA) operating in gain saturation was reported highlighting the effects of the relative phase of the signal and idler input waves on the gain and phase of the signal wave at the PSA output.

In this paper, we experimentally investigate and demonstrate for the first time to the best of our knowledge, a fiber-based all-optical switch using a PSA operated in saturation. We exploit the changes in the relative phase of the interacting input waves in a PSA to control the power of a strong (pump) wave. This PS all-optical switch can provide power extinction ratios of more than 30 dB and we believe that it potentially can work at very high speeds (>100 GHz). Consequently, this work substantially contributes towards the development of applications in the optical communications field allowing all-optical functionalities such as transistors or gates for signal processing.

This manuscript is organized as follows: Section 2 is composed of three subsections. In subsection 2.1, the principle of the phase-sensitive all-optical switch is presented. Furthermore, the setup implemented to experimentally demonstrate the optical switch is described in subsection 2.2. In subsection 2.3, the characterizations and the results are shown and discussed. Finally, section 3 contains the main conclusions derived from this work.

2. The phase-sensitive all-optical switch

In this section, we explain the basic concept for the implementation of the fiber-based phase sensitive all-optical switch. It is followed by the experimental setup implemented for its demonstration, as well as the results obtained.

2.1 Principle

In order to understand the principle of the all-optical switch based on phase-sensitive parametric amplification, it is worth mentioning concepts of some other basic parametric processes related to the one from which the optical switch is conceived. To do so, Fig. 1(a) illustrates the well-known single-pump phase-insensitive (PI) parametric amplification scheme. In a PI amplifier two interacting waves at different frequencies, one of high optical power (called the pump, at ω_p) and one of low optical power (called the signal, at ω_s) co-propagate in a HNLF. Through a FWM process another wave (called the idler) is created at a frequency of ω_i given by $\omega_i = 2\omega_p - \omega_s$. The result is having the three waves at the output of the PI with correlated phases. The relative phase (θ_{rel}) defined as $\theta_{rel} = 2\theta_p - \theta_s - \theta_i$, with θ_p , θ_s and θ_i being the phases of the pump, signal and idler waves, respectively, determines the phase matching condition which allows an efficient parametric amplification of the signal and idler

waves at the PI output. In a PI amplifier, the idler wave is generated so that θ_{rel} is constant and the PI gain in the saturated regime is only dependent on the power of the interacting waves so that the output pump power $P_{p_out}(P_{s_in})$ changes with the input signal power. This mechanism was used in [16–18]. In a PSA, see Figs. 1(b) and (c), at least three interacting and phase correlated waves are required at the HNLF input [21–23]. An important parameter to consider is that the optical powers of the signal and idler waves should be nearly equal in order to maximize the efficiency of the phase-sensitive process. Since the gain is phase sensitive, changes in the relative phase are converted into intensity changes, and in saturation, the output pump power is dependent on the power and phases of the interacting waves, expressed as $P_{p_out}(P_{s,i_in}, \theta_{rel})$. On the one hand, the PSA can be operated in the small-signal regime (unsaturated), see Fig. 1(b). In this case, the signal and idler waves will be equally amplified and depletion of the pump does not take place. On the other hand, when the powers of the interacting waves are sufficiently high at the input of the PSA, the gain is saturated. This condition can lead to the depletion of the pump wave, see Fig. 1(c). By controlling the θ_{rel} among the three interacting waves at the PSA input, it is possible to control the flow of power to or from the pump. This is the principle of the all-optical switch presented in this manuscript. More specifically, it means that by changing the phase of one or more of the waves at the input of the PSA the θ_{rel} can be set to any arbitrary value. In this study, we change the θ_{rel} by adding θ_{mod} to the phases of the signal and idler waves, i.e. $\theta'_s = \theta_s + \theta_{mod}$ and $\theta'_i = \theta_i + \theta_{mod}$, respectively. This idea is illustrated in Fig. 1(c). Depending on the value of the θ_{rel} , set by the phase variation of the signal and idler waves at the PSA input, the direction of the power flow is controlled, resulting in an efficient control of the PSA output pump power. From the work reported in [22], we expect that a phase change of the signal and idler waves of $\pi/2$ rad will cause a change in the θ_{rel} of π rad, resulting in maximum to minimum phase-sensitive gain with, in saturation, a concomitant pump power fluctuation at the PSA output.

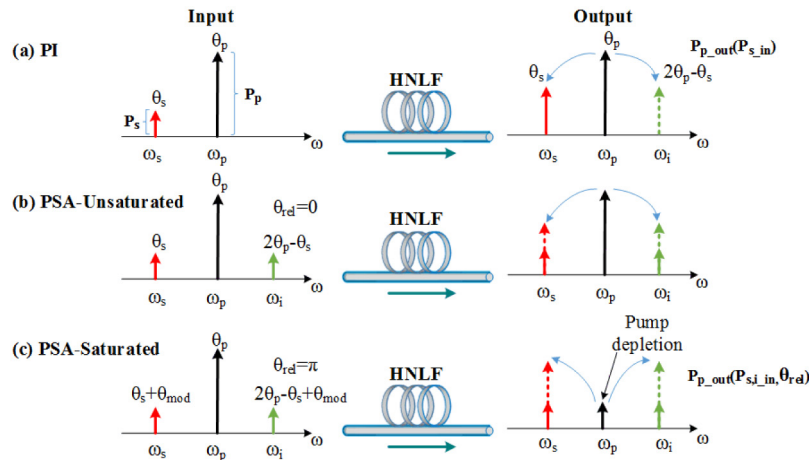


Fig. 1. Illustration of the basic principle of the phase-insensitive and phase-sensitive processes governing the fiber-based all-optical switch concept.

2.2 Experimental setup

In order to study the effects of the phase variation of the signal and idler waves on the pump power at the PSA output, an experimental setup was built for this purpose as depicted in Fig. 2. The pump source (laser 1) is a tunable laser (linewidth <100 kHz) set at a wavelength of 1554.1 nm. The pump wave was phase modulated using one radio-frequency (RF) tone at 300 MHz (PM1). In the experiment presented here, only one RF tone was used to increase the stimulated Brillouin scattering (SBS) threshold, which enables the necessary output powers

and gains for the involved waves used in the FOPA stages. Subsequently, the pump at the PM1 output was boosted by a high-power erbium doped fiber amplifier (EDFA-1). An optical band-pass filter (OBPF-1) with 2 nm bandwidth was used to reduce the amplified spontaneous emission (ASE) generated by the EDFA-1. The signal source (laser 2) consisted of another tunable laser set at a wavelength of 1550.8 nm. Both signal and pump were joined and launched into a well-known copier configuration [23] in order to generate a phase correlated idler wave through a FWM process at a wavelength of 1557.4 nm. The copier comprised a HNLf of 500 m length, with ZDW of 1541.1 nm, nonlinear coefficient (γ) of $11.5 \text{ (W} \cdot \text{km)}^{-1}$, polarization mode dispersion (PMD) with a differential group delay (DGD) of 0.05 ps, and a dispersion slope of $0.019 \text{ ps / (nm}^2 \cdot \text{km)}$. The gain of the copier was 3 dB.

The three phase-locked waves from the copier output (signal, idler and pump) were passed through a wavelength division multiplexer (WDM) coupler to separate the pump wave from the signal/idler pair. The powers of the signal/idler pair were amplified (EDFA-2) and sent to a waveshaper (WS) by which the desired amplitudes can be set. In addition, the WS provided a very narrow filtering of the signal/idler waves, removing any residual ASE from EDFA-2. To sweep the signal/idler phases over all states phases, a phase modulator (PM2) driven by a triangular waveform from an arbitrary waveform generator (AWG) was used. The pump wave coming out from the copier was further amplified to provide the necessary power at the PSA input. The relative phase between the pump and signal/idler pair was stabilized from thermal drift and acoustic noise using a phase-locked loop (PLL) based on a frequency dithering technique. The frequency dithering was applied using a piezoelectric transducer (PZT)-based fiber stretcher placed in the pump path. The pump was recombined with the signal/idler pair with another WDM (WDM-3) coupler and injected into the PSA. The PSA was implemented with a cascaded fiber with a total length of 586 m which is composed of four pieces of standard HNLf of different lengths, with nonlinearity coefficient of $9.7 \text{ (W} \cdot \text{km)}^{-1}$. All fiber pieces are separated by isolators and have a strain gradient applied (which was achieved by spooling the four fiber pieces with a controlled tension gradient) to change their individual SBS downshifts and increase the overall threshold. This fiber is an improved version of the fiber used in [24]. Polarization controllers (PC-5 and PC-6) were used to align the state of polarization of the waves at the PSA input. At the PSA output, a 99/1 optical coupler and a WDM (WDM-4) coupler allowed to recover the PSA output waves, either altogether or the pump separated from the signal and idler waves. Optical filters were placed for a better wave selection before being photodetected and analyzed with an optical sampling oscilloscope. Complementary measurements and analyses of the PSA output waves were performed with an optical spectrum analyzer (OSA). Monitoring taps were available before and after the copier and PSA stages. The setup shown in Fig. 2 is the general setup for the full characterization of the phase-sensitive all-optical switch. However, it also provides the components to implement the PI measurements as well as for a static characterization of the switch. For PI measurements (no idler is present), the signal and pump powers at the WDM-1 coupler are sent to the input of the (99/1-3-) coupler which is connected to HNLf comprising the PSA, as shown in Fig. 2. For the static characterization of the PSA all-optical switch, a small modification of the setup shown in Fig. 2 was performed. There was no need for using a PLL since the dual-path (or interferometric) stage was bypassed and the three phase correlated waves (signal, idler and pump) from copier passed a single path. The three waves were sent to a WS followed by a high power EDFA-2 in cascade with a bandpass filter with 6 nm bandwidth and a PC before their injection into the PSA stage. The WS allowed setting the desired relative amplitudes and phases of the interacting waves at the PSA input.

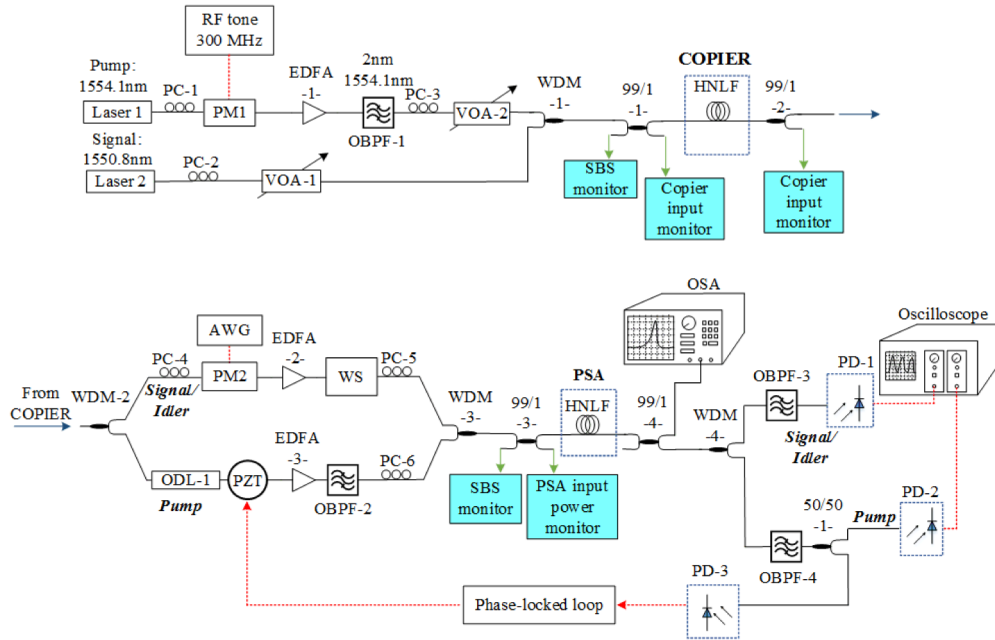


Fig. 2. Experimental setup. The acronyms are explained in the text. Black lines represent optical connections. Red-dashed lines represent electrical connections.

2.3 Characterizations and measurement results

Before describing and analyzing any results in this subsection, it is worth mentioning that the pump and signal wavelengths used in the demonstration of the PSA all-optical switch have been selected after a series of multiple characterizations.

The first of these involved the determination of the bandwidth and gain necessary for the parametric amplification. In order to do that, the fluorescence spectrum was obtained by setting the pump wavelength at different positions in the anomalous dispersion region of the fiber, while characterizing the bandwidth and gain. This characterization was very important as the bandwidth of the fluorescence spectrum determined the wavelengths that were to be used in the experiments. This allowed us to generate and manipulate the signals of interest with the available laboratory equipment, while maintaining the necessary amount of gain for the parametric process to be efficient.

The second set of characterizations were the analysis of the parametric amplifier in the PI mode, which means that no idler wave was present at the input of the PSA. It involved setting the wavelength of the pump wave at certain values (imposed by the fluorescence characterization), then for each pump wavelength several different pump powers values were used. In addition, for each combination of pump power-wavelength a wavelength scan of the signal wave was performed. It has been demonstrated that high pump depletion can be achieved in a fiber-based PIA [25], and that was the main reason for starting with the PI characterization. From the PI characterization, a combination of pump power/wavelength and the signal wavelength that provides the largest pump power depletion were selected to be 1554.1 nm / 32.2 dBm, and 1550.8 nm, respectively. This gave a pump power depletion ER of 34.2 dB. Figure 3(a) shows the variation of the PI output pump power as a function of the input (signal) power. From Fig. 3(a), we find that a minimum pump power of -5.8 dBm is achieved when an input signal power of 1.6 dBm is injected into the PI. A maximum pump power of 28.4 dBm is achieved and remained constant in the small signal region (i.e., the unsaturated-gain region) when less than -13 dBm of signal power is injected. For this

measurement, we define the pump depletion extinction ratio (ER) as the ratio of the output pump power in the presence and in the absence of the wave (in the PI case, the signal input power) at the input of the PI. In this context, a pump depletion extinction ratio of 34.2 dB (99.96%) is obtained which, incidentally, is the highest pump depletion ever reported in a PIA, to the best of the authors' knowledge. The wavelength parameters also agree with the theory presented in [26] where the signal wavelength that best deplete the pump is predicted in the vicinity of a half the spectral distance between the pump and the peak gain wavelengths.

Now, since we aim to investigate a PSA (with the idler present), a third characterization-stage implicated extending the power characterizations to the PSA case in order to determine the signal and idler powers inducing the maximal output pump depletion ER. In order to do that, the setup shown in Fig. 2 was utilized and the power of the signal/idler pair was varied, while the pump power was kept constant to 32.2 dBm, with the subsequent analysis of the waves at the output of the PSA with the OSA. The phase relation among the interacting waves at the PSA input is governed by the copier output (which gives $\theta_{\text{rel}} = 0$) and is preserved as stable as possible by the PLL. Figure 3(a) shows the PSA output pump power as a function of the input power. In the PSA case, the label "input power" found in Figs. 3 accounts for the individual average power (not the sum of their individual powers) of the signal and idler injected into the PSA. From Fig. 3(a), it is observed that a minimum pump power of -2 dBm is attained when individual input signal and idler powers of -0.4 dBm are injected into the PSA. A maximum pump power of 28.4 dBm is achieved and remains constant in the small-signal region, when less than -15 dBm of the signal and idler powers are injected. For this characterization, a pump depletion extinction ratio of 30.4 dB (99.91%) is obtained. The difference in the ERs between PI and PSA is mainly due to the imperfect stability of the PLL used in the PSA setup to compensate for the thermal drifts and acoustic noise. At the point of maximal depletion, many higher order idlers were generated forming a comb-like spectrum covering 100 nm. We emphasize that the creation of such higher order idlers is unavoidable due to the necessary placement of the signal wavelength to achieve a high ER [27]. At least fifteen created modes had a power-to-noise ratio >20 dB. Optical frequency combs based on HNLF have been investigated in other contexts, and it has been demonstrated that they can cover 200 nm bandwidth [28]. Figure 3(b) illustrates such an optical spectrum, taken over a span of 50 nm with a resolution of 0.5 nm. Also, the optical spectrum of the PSA output when no signal/idler pair is injected into the PSA is shown. From Fig. 3(b), we can observe the asymmetric optical spectrum with the higher order idler components.

The pump OSNR at the PSA input was >52 dB; and OSNRs for the signal and idler were of more than 46 dB. The small signal (unsaturated) gain was of around 28 dB. Moreover, the output powers of the signal and idler waves at the PI and PSA output can be quantified as a function of their respective input powers, as shown in Fig. 3(c). The signal and idler output powers increase linearly with the signal (and idler) input powers for the PI (PSA) case, and remain like that until the saturation threshold is reached at around -4 dBm (-6 dBm). From these points and as the input powers are further increased, the idler power gets higher than the corresponding power of the signal wave. Subsequently, as the signal (PI case) and signal and idler (PSA case) reach the corresponding input powers of 1.6 dBm and -0.4 dBm, the pump power is decreased at the point of maximum depletion. In this saturation region, the phase matching condition is modified and the energy is greatly transferred from the pump to the higher order idlers. The asymmetry between the output signal and idler powers in the region of high input power is mainly due to two facts: the dispersion of the fiber, which greatly enhances the idler over the signal wave, as well as for the Raman-induced power-transfer characteristics among the interacting input waves [22,27,29]. These higher order idlers do not affect the final goal for the demonstration of the optical switch as the pump can be filtered out and utilized accordingly. The value of the ER depends on the degree of saturation of the PSA, and by the gain of the PSA as a result of the pump power applied. Particularly, considering

the parameters of power and wavelengths of the interacting waves at the PSA input treated in the current manuscript, the ER is determined from the values of the signal and idler powers that produce a reduction of 3 dB in the output pump power to the maximal pump depletion.

Next, the evaluation of the PSA and its switching potential by changes in the relative phase among the interacting waves at its input was performed. For this investigation, the setup shown in Fig. 2 was modified according to the description provided at the end of subsection 2.2 for the static characterization. This setup modification was necessary since that slow changes in the phase of the waves at the PSA input (with the WS) would be compensated by the PLL and giving erroneous results. Since a 6 nm filter allowed not only to pass the three interacting waves but also some ASE from the EDFA before it, the power for the signal and idler had to be adjusted at the PSA input to -2.3 dBm for a pump power of 32.2 dBm. In addition, the maximal ER achieved with this setup was of 21.5 dBm when performing a measurement of output power as a function of input power. Then, the signal and idler powers at these values where the maximum depletion was encountered were kept fixed, and the relative phase of the signal and idler waves was varied with the WS. The pump, signal and idler powers at the PSA output as a function of the input signal and idler phase are shown in Fig. 3(d) in linear (mW) scale. From this figure, we can observe that at the point of maximal pump power depletion half of the pump power is transferred to the idler and that around 20% of the pump power goes to the signal. The remaining power is distributed among the generated higher order idlers. In addition, a periodic phase dependence of the pump power at the PSA output is obtained, and the maximum to minimum values are reached by changing the phase of the signal and idler waves $\pi/2$ rad (causing changes in the relative phase of π rad). This result matches our expectations as it was described previously in subsection 2.1. At this point, we redefine the ER (for the phase-sensitive all-optical switch concept) as the output pump power change as a function of the relative phase variation. The ER of the optical switch found through this static characterization is 22.4 dB. The ER difference when comparing the output pump power as a function of the input power and as a function of the relative phase variation is mainly due to the different schemes used, and also limited by the ASE contribution of the EDFA to the PSA input in the static characterization setup. Although, taking into account the theory provided in [26] about the power conservation in parametric amplifiers, we would expect having the same ER value when the power or the phase of the signal and idler is varied in a PSA. This is also confirmed when analyzing the traces shown in Fig. 3(d). The pump power under depletion is distributed among the signal and idler waves as well as the higher order idlers.

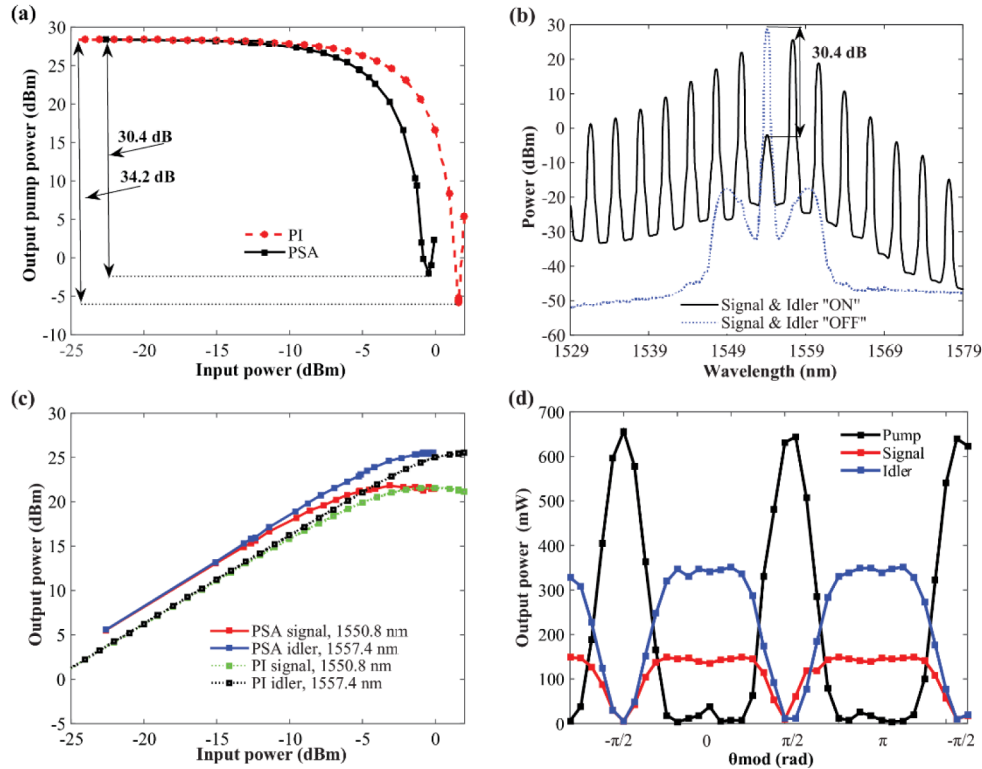


Fig. 3. (a) Output pump power vs. input power, PI (red) and PSA (black); (b) optical spectra at the output of the PSA for an input signal and idler power of -0.4 dBm, and without any input wave; (c) input signal/idler power vs. output signal/idler power, PI and PSA cases; (d) PSA output power vs phase variation of the signal and idler waves.

Finally, considering the results provided by the static characterization, the following experiment was to dynamically change the phases of the signal and idler waves at the PSA input and analyzing their effect on the output pump power. The setup utilized for this assessment was, again, the one shown in Fig. 2. The combination of powers and wavelengths of the input waves (signal, idler and pump) that resulted in the maximal pump depletion in the PSA static characterization was used. In the setup shown in Fig. 2, a triangular signal at 100 MHz drove the phase modulator (PM2) placed in the signal/idler path. The frequency of this signal was selected due to the electrical components involved in its generation (RF amplifiers and AWG) ensuring a well-defined triangular waveform driving the phase modulator. This signal allowed smooth changes of the signal and idler phases (by adding θ_{mod}), as θ_{mod} varied progressively from $-\pi$ rad (the lowest amplitude of the triangular signal) to zero (at half the amplitude of the triangular signal) and from zero to π rad (the highest amplitude of the triangular signal), back and forth. Figure 4. shows time traces of the triangular signal (dotted-blue line), and of the output pump power (continuous line), in a period of 10 ns. From the figure, we can verify that a maximum pump power is periodically found every π rad. Moreover, every $\pi/2$ rad we observe a maximum and a minimum pump power. The shape of the pump trace represented in Fig. 4, illustrates very well the switching functionality performed by the PSA. It is worth noticing that, since the optical switching occurs very fast, it is not possible to analyze it with an OSA, but instead the oscilloscope must be used, which limits the dynamic range. The PD has a dynamic sensitivity range of 19 dB, which limits the precise representation of the expected 30 dB pump depletion ER. For the trace shown in Fig. 4, the pump ER is around 16 dB, since we limited the power injected into the PD for safety reasons.

The maximum power of the pump trace shown in Fig. 4 is of 187 mW. In addition, the pump trace in Fig. 4 confirms the expected optical switching behavior presented in subsection 2.1. If the real extinction ratio of this optical switch was possible to measure in the temporal domain, we would expect to see a sharper pulse which would mean having an efficient power/phase ratio. Nevertheless, Fig. 4 clearly demonstrates the potential of the PSA to achieve a fast and efficient all-optical switching of a strong signal controlled by the phase of the interacting waves.

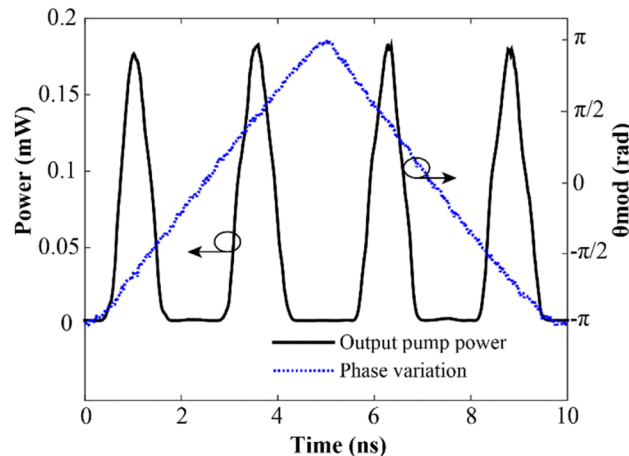


Fig. 4. Time traces: PSA output pump, amplitude and power (continuous line); phase modulated variation (dotted line).

3. Conclusion

In this work, we have experimentally demonstrated an all-optical switch in a phase-sensitive fiber-based parametric amplifier. A highly nonlinear fiber was used as the nonlinear platform. The implemented setup enabled us to measure a high pump depletion ER, which was of 30.4 dB, meaning that a pump power depletion of 99.91% was attained. Before studying the PS case, an investigation of the bandwidth and gain was necessary to determine the parameters of power and wavelength that would allow to implement the setup followed by a PI characterization. The latter resulted in the demonstration of the highest pump depletion ever reported, with an impressive ER of 34.2 dB. After, the static characterization of the PS all-optical switch was assessed retrieving an ER of 22.4 dB, which was 8 dB below the expected value, mainly due to extra ASE from an EDFA added at the PS input. Moreover, the phase-sensitive all-optical switch was dynamically demonstrated at a speed of 100 MHz. The behavior of the pump power measured as a function of the modulated phase variations on the signal and idler provided evidence of the periodic pump power variation every π rad, as well as that a change of $\pi/2$ rad results in obtaining the maximal pump depletion. Owing to the ultrafast nonlinear nature of the process that gives rise to parametric amplification it is expected that the switch operates at very high rates. In spite of having a high pump power (1.6 W) for the saturation of the PSA based on silica HNLF, we note that this concept can be applied to other platforms with higher nonlinear coefficient and potentially a higher conversion efficiency. This would result in a considerable reduction in the input power requirements for the saturation of the PSA to develop a PS all-optical switch and facilitating its integration for real applications.

The parameters of power and wavelength of the PSA input waves are not restricted to the ones used in this manuscript. Rather, they would depend on the desired application but taking into account the bandwidth and gain desired for a maximal efficiency of the parametric process. This makes our proposed PS all-optical switch reconfigurable, at the expense of

extinction ratio. As mentioned in subsection 2.3, the current parameters were selected based also on the availability of laboratory equipment, but the idea can be applied in a wide range of wavelengths depending on the application and mainly limited by the requirement of gain and bandwidth required for its implementation. As a result, the research presented in this manuscript demonstrates the potential of a phase-sensitive all-optical switch as another solution in the development of new all-optical devices and functionalities in the optical communications field.

Acknowledgments

This work is supported by the European Research Council under grant agreement ERC-2011-AdG - 291618 PSOPA and by the K. A. Wallenberg Foundation.